

# A 2-level system of cold sodium atoms with high and tunable susceptibility against the magnetic field

Z. B. Li, D. X. Yao, Y. Z. He, and C. G. Bao\*

*The State Key Laboratory of Optoelectronic Materials and Technologies  
School of Physics and Engineering, Sun Yat-Sen University, Guangzhou, P. R. China*

A 2-level spin-system of cold sodium atoms is proposed. Both the cases that the system has arrived at thermo-equilibrium and is in the early stage of evolution have been studied. This system is inert to the magnetic field  $B$  in general but very sensitive in a narrow domain around  $B = B_0$ , where  $B_0$  can be predicted and is tunable. A characteristic constant  $\gamma = 0.278466$  dedicated to various 2-level systems is found, and leads to an upper limit for the internal energy  $U$  of the whole system so that  $U \leq \gamma k_B T$ . This limit is considerably lower than the energy assigned to the spatial motion of only a single particle. Under thermo-equilibrium, the populations of spin-components measured at distinct  $T$  converge to a fixed value when  $B = B_0$ . The period and amplitude of population oscillation are found to be seriously affected by the special sensitivity against  $B$ . Rich messages on the dynamic parameters could be obtained via experimental measurements of these systems.

PACS numbers: 03.75.Hh, 03.75.Mn, 03.75.Nt

It is widely believed that the systems of cold atoms are promising in application.[1] Among them the 2-level systems are notable because the quantum bit might be thereby defined. In this paper a 2-level system of cold sodium atoms defined in pure spin-space is studied. This system is inert to the magnetic field  $B$  in general but very sensitive in a specific domain of  $B$ . The location of the domain is tunable. The features of the system under thermo-equilibrium and in the early stage of evolution [2–9] have both been studied. A characteristic constant  $\gamma = 0.278466$  is found, and accordingly the internal energy  $U$  of the whole system relative to its ground state (g.s.)  $\leq \gamma k_B T$  disregarding to the particle number  $N$  and the details of dynamic parameters. The above upper limit for  $U$  is considerably smaller than  $\frac{3}{2}k_B T$ , the energy assigned to the spatial motion of only a single particle. Thus the energy involved in the system is extremely low. The population oscillation is found to be seriously affected by the special sensitivity against  $B$  of the system.

Let  $N$  spin-1 sodium atoms be trapped by an isotropic harmonic potential  $\frac{1}{2}m\omega^2 r^2$ . When  $B$  is not applied, the Hamiltonian

$$H = \sum_i \left( -\frac{1}{2}\nabla_i^2 + \frac{1}{2}r_i^2 \right) + \sum_{i<j} \delta(\mathbf{r}_i - \mathbf{r}_j) (c_0 + c_2 \mathbf{f}_i \cdot \mathbf{f}_j) \quad (1)$$

where  $\mathbf{f}_i$  is the spin-operator of the  $i$ -th particle,  $\hbar\omega$  and  $\sqrt{\hbar/m\omega}$  have been used as units for energy and length. We assume that all the spatial degrees of freedom are frozen (the condition that this assumption is realized is given below). Note that the interaction keeps the total spin  $S$  and its component  $M$  conserved. Thus the eigenstates can be written as  $\Psi_{SM} = \prod_{i=1}^N \phi_S(\mathbf{r}_i) \vartheta_{SM}^N$ , where  $\vartheta_{SM}^N$  is the normalized all-symmetric spin-state with the

good quantum numbers  $S$  and  $M$ . It has been proved that  $\vartheta_{SM}^N$  is unique and  $N - S$  must be even. [10, 11] The concrete form of  $\vartheta_{SM}^N$  is irrelevant because related calculations can be performed by using the fractional parentage coefficients.[12] Inserting  $\Psi_{SM}$  into the many-body Schrödinger equation, the equation for  $\phi_S(\mathbf{r})$  is [11]

$$\begin{aligned} & \left\{ \hat{h}_0 + [(N-1)c_0 + \frac{S(S+1) - 2N}{N}c_2] |\phi_S|^2 \right\} \phi_S(\mathbf{r}) \\ & = \varepsilon_S \phi_S(\mathbf{r}) \end{aligned} \quad (2)$$

Where  $\hat{h}_0 = -\frac{1}{2}\nabla^2 + \frac{1}{2}r^2$  is the Hamiltonian of a single particle in the trap. Accordingly, the energy of  $\Psi_{SM}$  is  $E_S = \int |\phi_S(\mathbf{r})|^4 d\mathbf{r} \left( \frac{N(N-1)}{2}c_0 + \frac{S(S+1) - 2N}{2}c_2 \right)$ .

When  $B$  is applied,  $S$  is no more conserved, but  $M$  is. For a  $M$ -conserved system the linear Zeeman term is irrelevant, thus the Hamiltonian arising from the magnetic field is

$$H_B = q \sum_i \mathbf{f}_{iz}^2 \quad (3)$$

where  $q = \mu_B B^2 / (\hbar^2 E_{HFS})$  and  $E_{HFS}$  is the hyperfine splitting. One can use the set  $\Psi_{SM}$  (with a fixed  $M$ ) to diagonalize  $H_B$ . The related matrix elements can be obtained by using the fractional parentage coefficients as [13]

$$\langle \vartheta_{S'M}^N | H_B | \vartheta_{SM}^N \rangle = Nq \sum_{\mu} \mu^2 q_{S'S}^{NM\mu} \quad (4)$$

where

$$\begin{aligned} q_{S'S}^{NM\mu} & = \delta_{S'S} [(a_{SM\mu}^{\{N\}})^2 + (b_{SM\mu}^{\{N\}})^2] \\ & + \delta_{S',S-2} a_{S-2,M\mu}^{\{N\}} b_{SM\mu}^{\{N\}} \\ & + \delta_{S',S+2} a_{S+2,M\mu}^{\{N\}} b_{SM\mu}^{\{N\}}. \end{aligned} \quad (5)$$

$$a_{SM\mu}^{\{N\}} = C_{1\mu, S+1, M-\mu}^{SM} \sqrt{\frac{(N-S)(S+1)}{N(2S+1)}} \quad (6)$$

\*Corresponding author: stsbcg@mail.sysu.edu.cn

$$b_{SM\mu}^{\{N\}} = C_{1\mu, S-1, M-\mu}^{SM} \sqrt{\frac{S(N+S+1)}{N(2S+1)}} \quad (7)$$

In the last two equations the Clebsch-Gordan coefficients have been introduced,  $\mu = \pm 1$  or  $0$  denotes the spin-component of a particle. After the diagonalization, the eigenstates can be obtained as  $\Psi_{i,M}^B = \sum_S d_S^{B,i} \Psi_{SM}$ , where  $i$  is a serial number ( $i = 1$  for the lowest).

We are interested in the systems with  $M$  fixed at  $N - 2$ . This is a 2-level system contains only two basis functions  $\Psi_{N-2,M}$  and  $\Psi_{N,M}$ . Their spatial wave functions  $\phi_{N-2}(\mathbf{r}_i)$  and  $\phi_N(\mathbf{r}_i)$  are very close to each other ( $\langle \phi_{N-2} | \phi_N \rangle > 0.999$ ). Therefore we omit their difference and set  $\phi_{N-2} = \phi_N = \phi$ . Dropping the terms that do not depend on  $S$ , then  $E_S = c \frac{S(S+1)}{2}$ , where  $c = c_2 \int |\phi(\mathbf{r})|^4 d\mathbf{r}$ . The matrix-equation for diagonalizing  $H + H_B$  is 2-dimensional, it is

$$H_{11}d_1 + H_{12}d_2 = Ed_1 \quad (8)$$

$$H_{21}d_1 + H_{22}d_2 = Ed_2 \quad (9)$$

Where  $d_1$  ( $d_2$ ) is the coefficient of  $\Psi_{N-2,M}$  ( $\Psi_{N,M}$ ). By using Eq.(4),  $H_{11} = \frac{c}{2}(N-2)(N-1) + q \frac{2N^2 - N - 2}{2N-1}$ ,  $H_{22} = \frac{c}{2}N(N+1) + q \frac{4N^3 - 4N^2 - 7N + 12}{(2N-1)(2N+3)}$ ,  $H_{12} = H_{21} = q \frac{2\sqrt{2N-2}}{(2N-1)}$ , where  $c$  can be obtained after Eq.(2) has been solved. The solutions of Eqs.(8) and (9) is straight forward. Both the eigen-energy  $E_i$  and the eigen-state  $\Psi_{i,M}^B = d_1^{B,i} \Psi_{N-2,M} + d_2^{B,i} \Psi_{N,M}$  have analytical forms. In particular, the energy gap  $E_{gap} \equiv E_2 - E_1 = \sqrt{(H_{11} - H_{22})^2 + 4H_{12}^2}$ . In what follows the subscript  $M$  will be dropped because  $M = N - 2$  is fixed.

We first study the susceptibility of the two eigenstates against  $B$ . The fidelity susceptibility is defined as [14]

$$\Gamma_i(B) \equiv \lim_{\varepsilon \rightarrow 0} \frac{2}{\varepsilon^2} (1 - |\langle \Psi_i^{B+\varepsilon} | \Psi_i^B \rangle|) \quad (10)$$

For Na,  $\Gamma_i(B)$  of the g.s. distinct in  $N$  are plotted in Fig.1. Due to the fact that  $d_1^{B,2} = -d_2^{B,1}$ , and  $d_2^{B,2} = d_1^{B,1}$ ,  $\Gamma_2(B) = \Gamma_1(B)$ , i.e., both states have exactly the same susceptibility. This is a spacial feature dedicated only to 2-level systems. There are sharp peaks in Fig.1 implying that the system is inert to  $B$  in general, but extremely sensitive when  $B$  falls in the specific narrow domains, namely, the domain of sensitivity (D-o-S). The location of the peak is denoted as  $B_{peak}$  which varies with  $N$  and/or  $\omega$ . The left and right borders of the D-o-S are named  $B_{left}$  and  $B_{right}$ . They can be roughly defined as  $\Gamma_i(B_{left}) = \Gamma_i(B_{right}) = \frac{1}{10} \Gamma_i(B_{peak})$ . A larger  $N$  will lead to a higher and narrower peak shifted to the right, while a larger  $\omega$  will lead to a lower and broader peak also shifted to the right.

$E_{gap}$  is plotted in Fig.2. For each  $N$ ,  $E_{gap}$  has a minimum located at  $q_0$  ( $B_0$ ). From  $\frac{dE_{gap}}{dq} = 0$ ,

$$q_0 = \frac{c(8N^2 - 18)}{4(2N + 3)} \quad (11)$$

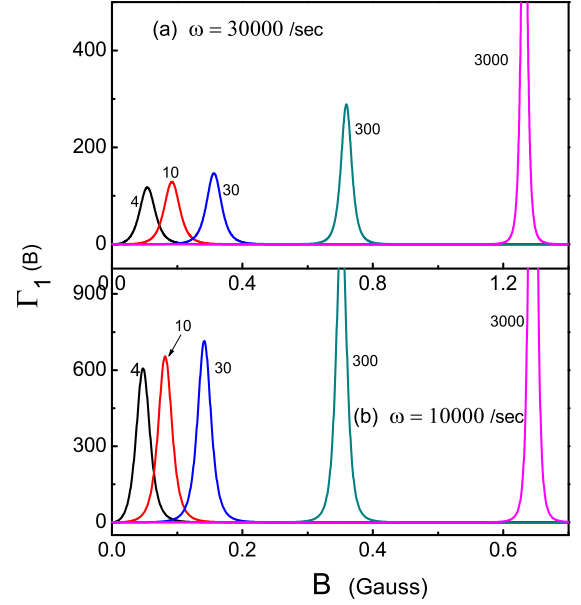


FIG. 1: (color on line) The fidelity susceptibility  $\Gamma_1(B)$  of the g.s. of the 2-level system of Na versus  $B$ .  $\omega = 30000 \text{ sec}^{-1}$  (a) and  $10000 \text{ sec}^{-1}$  (b), and  $N$  is given at five values marked by the curves. Note that the scales of  $B$  are different in (a) and (b).

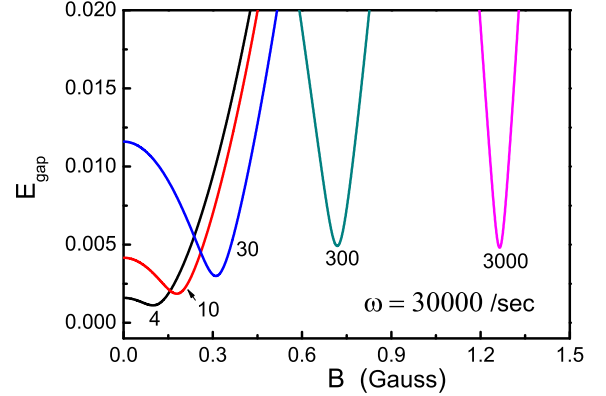


FIG. 2:  $E_{gap}$  of the 2-level system versus  $B$ .  $\omega = 30000 \text{ sec}^{-1}$  is assumed. Refer to Fig.1a.

(for Na,  $q_0$  and  $B_0$  fulfill the relation  $q = 1745B^2/\omega$ , where  $q$  is in  $\hbar\omega$  and  $B$  is in *Gauss* [1]). By comparing Fig.2 and 1a, we found that  $B_0 \approx B_{peak}$ . They are closer to each other when  $N$  is larger (say,  $B_{peak} - B_0 = 0.0096$ ,  $0.0003$ , and  $0$  when  $N = 4$ ,  $300$ , and  $3000$ , respectively). In fact, when we expand  $\Psi_i^{B+\varepsilon}$  via a perturbation series, we found that  $\Gamma_i(B) \propto (E_{gap})^{-2}$ , thus a smaller gap will lead to a higher sensitivity. Eq. (11) explain why a larger  $N$  will lead to a larger  $B_{peak}$ . Furthermore, a larger  $\omega$  will lead to a more compact  $\phi(\mathbf{r})$ , and therefore a larger  $c$  and a larger  $B_{peak}$  as well. Eq.(11) provides a convenient way to evaluate the location of the D-o-S. When  $N$  is large, under the Thomas-Fermi approximation,  $c \propto (\omega^2/N)^{3/5}$ .

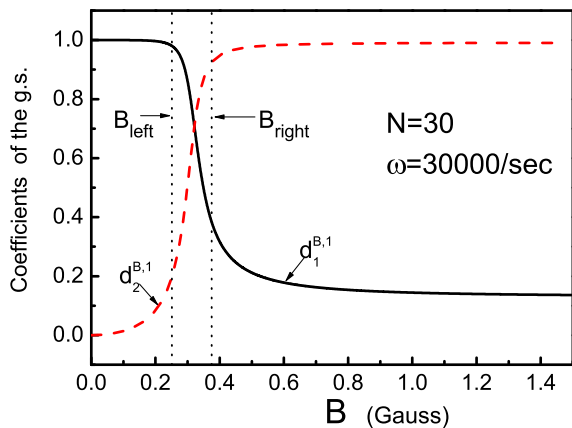


FIG. 3: The coefficients  $d_1^{B,1}$  (solid) and  $-d_2^{B,1}$  (dash) of the g.s. versus  $B$ .  $N = 30$  and  $\omega = 30000/\text{sec}$  are assumed.

Accordingly,  $B_0 \propto (\omega^3 N)^{1/5}$ . Thus  $B_0$  increases with  $N$  slowly but increases with  $\omega$  rapidly as shown in Fig.1.

The variation of the g.s. versus  $B$  is shown in Fig.3. The D-o-S appearing in Fig.1a appears again in Fig.3, wherein the coefficients  $d_1^{B,1}$  and  $d_2^{B,1}$  undergo a sharp change. When  $B < B_{\text{left}}$ ,  $d_1^{B,1}$  remains  $\approx 1$  implying that the effect of  $B$  is effectively hindered by the gap. When  $B > B_{\text{right}}$ , we found that  $\Psi_1^B \rightarrow \Pi_{i=1}^N \phi(\mathbf{r}_i) \|N-2, 2, 0\rangle$ . Where  $|N_1, N_0, N_{-1}\rangle$  is a Fock-state in the spin-space having  $N_\mu$  particles in  $\mu$ . Note that, when  $B \rightarrow \infty$ ,  $N_0$  in a g.s. should be maximized (under the conservation of  $M$ ) to reduce the quadratic Zeeman energy. Therefore,  $\Psi_1^B$  should tend to the above limit. Whereas the excited state  $\Psi_2^B \rightarrow \Pi_{i=1}^N \phi(\mathbf{r}_i) \|N-1, 0, 1\rangle$ . From Fig.3 we know that, when  $B$  increases, the spin-state of the g.s. is changed from  $\vartheta_{N-2, M}^N$  to  $|N-2, 2, 0\rangle$  and the change happens essentially inside the D-o-S. Accordingly, matching the change of the g.s., the excited state is changed from  $\vartheta_{N, M}^N$  to  $|N-1, 0, 1\rangle$ .

When the system has arrived at thermo-equilibrium under a given temperature  $T$ . If  $T$  is very low, the spatial excitation is negligible and the system would be essentially distributed among the above two eigenstates. Since the energy for spatial excitation  $\approx 1$  (in  $\hbar\omega$ ), the ratio  $R_T \equiv e^{-\beta E_{\text{gap}}} / e^{-\beta}$  is crucial, where  $\beta = 1/(k_B T)$ . We define  $T_a$  and  $T_b$  at which  $R_T = 10$  and 100, respectively. When  $T < T_a$ , the effect of spatial excitation is small, when  $T < T_b$ , the effect of spatial excitation is negligible. Thus, when  $T < T_b$  the partition function of the system is simply  $Z \approx 1 + e^{-\beta E_{\text{gap}}}$ . The probability that the system lies at the g.s. is  $P_g = 1/Z$ . We define further a turning temperature  $T_1(B)$  at which  $P_g = 0.95$ . When  $T < T_1(B)$ , not only the spatial but also the spin degrees of freedom are nearly frozen. Thus  $T_1(B)$  marks the temperature of the secondary condensation.[15, 16] Let  $P_{ex} = e^{-\beta E_{\text{gap}}} / Z$  which is the probability lying at the excited state. Note that when  $T \rightarrow \infty$ , an ideal 2-level system would have  $P_{ex} \rightarrow 1/2$ . Thus we define the second turning temperature  $T_2(B)$  at which  $P_{ex} = 0.95 \times 1/2$ .

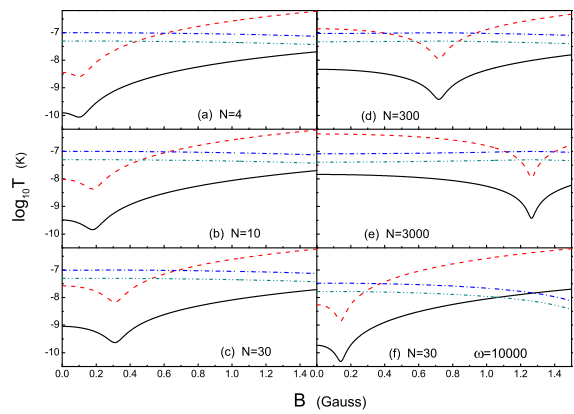


FIG. 4:  $T_1$  (solid),  $T_2$  (dash),  $T_a$  (dash-dot) and  $T_b$  (dash-dot-dot) versus  $B$ .  $\omega = 30000 \text{ sec}^{-1}$  (a to e) and  $10000 \text{ sec}^{-1}$  (f), and  $N$  is given at five values marked in each panel. In the zone below  $T_b$  the spatial excitation can be neglected. In the zone below  $T_1$  the system remains in the g.s.. In the zone between  $T_b$  and  $T_2$ , the thermo-fluctuation is saturated.

When  $T = T_2(B)$ , the thermo-fluctuation is close to be saturated. The variations of  $T_1(B)$ ,  $T_2(B)$  together with  $T_a$  and  $T_b$  versus  $B$  are plotted in Fig.4. From the definitions of  $T_1(B)$  and  $T_2(B)$ , one can prove that they will also arrive at their minimum at  $B_0$  as shown in Fig.4. When  $T$  is explicitly lower than  $T_b$ , the 2-level system can be safely considered as a pure spin-system.

The internal energy relative to the g.s. is

$$U(T, B) \equiv E_{\text{gap}} e^{-\beta E_{\text{gap}}} / Z = E_{\text{gap}} P_{ex} \quad (12)$$

When  $T$  is fixed,  $\frac{\partial U}{\partial B}$  would be zero if  $B = B_0$  and if  $e^{-\beta E_{\text{gap}}} - \beta E_{\text{gap}} + 1 = 0$ . For the latter case,  $E_{\text{gap}} = 1.27846 k_B T$  and  $U$  arrives at a maximum  $\gamma k_B T$ , where  $\gamma = 0.278466$  is a characteristic constant dedicated to 2-level systems disregarding  $N$ ,  $\omega$ , and the parameters of interaction. Note that  $\frac{3}{2} k_B T$  is the energy assigned to the spatial motion of only a single particle, while  $U$  is the total spin energy (relative to the g.s.). Thus the very small upper limit  $\gamma k_B T$  manifests how weak the energy is involved.

An example of  $U$  versus  $B$  (associated with Fig.4c) are plotted in Fig.5.  $T$  is given at three values,  $T_A = T_1(B_{\text{left}}) = 10^{-9.43} \text{ K}$ ,  $T_B = T_2(B_{\text{left}}) = 10^{-7.96} \text{ K}$ , and  $T_C = (T_A + T_B)/2$ . When  $T = T_A$  and  $B$  increases from  $B_{\text{left}} \rightarrow B_{\text{right}}$ , it is clear from Fig.4c that  $T_A - T_1(B)$  appears as a small peak. It implies that  $P_{ex}$  undergoes an increase and afterward a decrease. Accordingly,  $U$  is peaked in the D-o-S as shown by the solid line in Fig.5. Whereas when  $T = T_B$  and  $B$  from  $B_{\text{left}} \rightarrow B_{\text{right}}$ , the system will enter to the zone where the thermo-fluctuation is saturated, and therefore  $P_{ex}$  will remain unchanged. In this case the variation of  $U$  is largely contributed by  $E_{\text{gap}}$ . The dip in  $E_{\text{gap}}$  (refer to Fig.2) leads to the dip in  $U$  as shown by the dash curve in Fig.5. When  $B$  is larger, the increase of  $E_{\text{gap}}$  remains, and thereby  $U$  keeps increasing until it arrives at its upper limit  $\gamma k_B T$ .

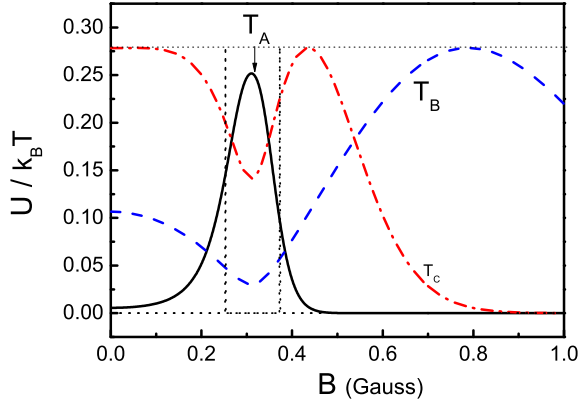


FIG. 5:  $U/k_B T$  versus  $B$ .  $N = 30$  and  $\omega = 30000/\text{sec}$  are assumed. The solid, dash, and dash-dot lines are for  $T = T_A$ ,  $T_B$ , and  $T_C$  (refer to the text), respectively. The two vertical dotted lines mark the D-o-S, and the horizontal dotted line marks the upper limit.

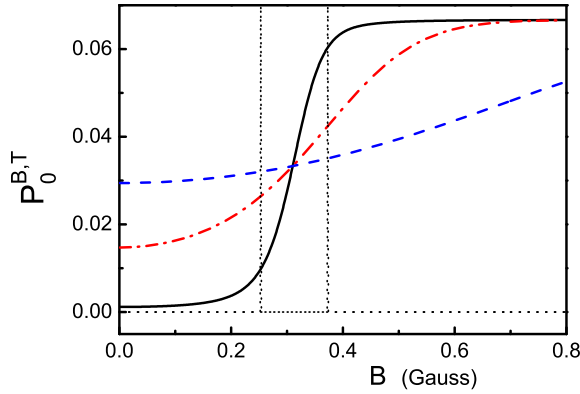


FIG. 6:  $\bar{P}_0^B$ , the weighted probability of a particle in  $\mu = 0$ , versus  $B$  for the case of Fig.4c. Refer to Fig.5.

When  $B$  is larger further, it is shown in Fig.4c that the system will tend to the g.s. so that  $U$  will tend to zero. It is notable that in all cases  $U \leq \gamma k_B T$  holds as shown by the horizontal dotted line.

The probability of a particle in  $\mu$  in the  $\Psi_i^B$  state, according to Eq.(9) of ref.[13], is

$$P_\mu^{B,i} = (d_1^{B,i})^2 q_{N-2,N-2}^{NM\mu} + (d_2^{B,i})^2 q_{N,N}^{NM\mu} + 2d_1^{B,i} d_2^{B,i} q_{N-2,N}^{NM\mu} \quad (13)$$

Taking the thermo-fluctuation into account, we define the weighted probability as

$$\bar{P}_\mu^{B,T} = (P_\mu^{B,1} + P_\mu^{B,2} e^{-\beta E_{gap}}) / Z \quad (14)$$

For the case of Fig.4c,  $\bar{P}_0^{B,T}$  is plotted in Fig.6, where  $\bar{P}_0^{B,T}$  changes sharply inside the D-o-S when  $T \approx T_A$ . Furthermore, it was found that  $P_0^{B_0,1} = P_0^{B_0,2} = 1/N$  when  $B = B_0$ . It arises because meanwhile the spin-state is equal to  $\frac{1}{\sqrt{2}}(|N-2, 2, 0\rangle \mp |N-1, 0, 1\rangle)$ , where  $-(+)$

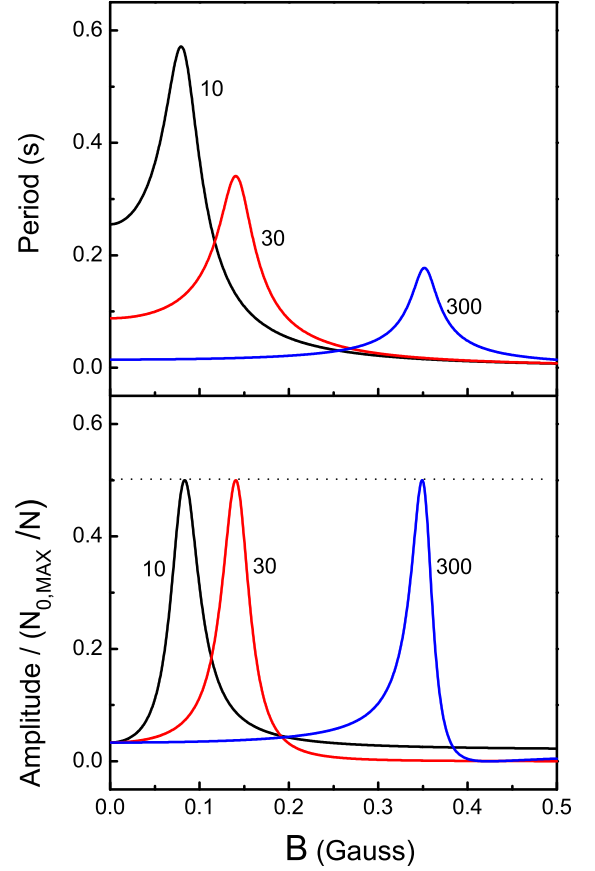


FIG. 7: Period (a) and the amplitude (b) of population oscillation of Na atoms versus  $B$ .  $\omega = 10000$  is assumed and  $N$  is given at three values marked by the curves. The unit of the amplitude is  $N_{0,MAX}/N$ , where  $N_{0,MAX} = 2$  is the maximal number of  $\mu = 0$  particles.

is for the g.s. (excited state). Therefore,  $\bar{P}_0^{B_0,T} = 1/N$  disregarding  $T$ . Accordingly, the three curves distinct in  $T$  converge at  $1/N$ . Once  $\bar{P}_0^{B,T}$  has been measured at distinct  $T$ , from the point of convergency one can know  $N$  and  $B_0$ , the latter is related to the dynamic parameters. When  $B$  is sufficiently large, from Fig.4, the system might fall into the g.s., and accordingly  $\bar{P}_0^{B,T} \rightarrow 2/N$  as shown in Fig.6.

There are a number of experiments related to the early stage of spin-evolution.[2–9] Starting from an initial state  $|\Psi_0\rangle$ , the system will evolve as  $\Psi(t) = e^{-iHt/\hbar}|\Psi_0\rangle = \sum_n e^{-iE_n t/\hbar} |n\rangle \langle n|\Psi_0\rangle$ , where  $E_n$  and  $|n\rangle$  denote the eigenenergy and eigenstate, respectively.[17] In general there are infinite eigenstates but only two for our two-level system. Thereby  $\Psi(t)$  has simple analytical form. Let the eigenstate be re-expanded by the Fock-states as  $\Psi_j^B = \prod_{i=1}^N \phi(\mathbf{r}_i) (b_1^{(j)} |N-2, 2, 0\rangle + b_2^{(j)} |N-1, 0, 1\rangle)$ ,  $j = 1, 2$ . Obviously,  $b_1^{(2)} = b_2^{(1)}$  and  $b_2^{(2)} = -b_1^{(1)}$ , they depend on  $B$ . When the initial state is so prepared that  $|\Psi_0\rangle = |N-1, 0, 1\rangle$  (Namely,  $N-1$  particles are prepared in spin up, then one down-particle is added), the

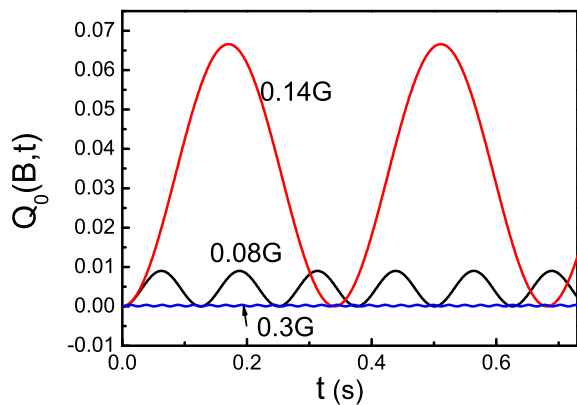


FIG. 8: Population oscillation  $Q_0(B, t)$  of Na atoms versus  $t$  (in sec).  $N = 30$  and  $\omega = 10000$  are given.  $B$  is given at three values marked by the curves (where,  $0.14G = B_0$ , refer to Fig.1b).

time-dependent probability of a particle in  $\mu = 0$  is [17]

$$Q_0(B, t) = A[1 - \cos(E_{gap}\omega t)] \quad (15)$$

where the amplitude  $A = \frac{4}{N}(b_1^{(1)}b_2^{(1)})^2$ . Eq.(15) provides a clear picture of population oscillation with the period  $t_p = \frac{2\pi}{E_{gap}\omega}$ . Examples on  $t_p$  and  $A$  are given in Fig.7. There are peaks in both 7a and 7b implying strong oscillation. They match exactly with the peaks in Fig.1b. However, outside the D-o-S, the amplitude is very small. When  $B = B_0$ ,  $|b_1^{(1)}| = |b_2^{(1)}| = \frac{1}{\sqrt{2}}$ , and therefore  $A = 1/N$ . and the number of  $\mu = 0$  particles  $N_0(t) \equiv NQ_0(B, t)$  oscillates from 0 to its maximum  $N_{0,MAX} = 2$  (refer to the horizontal dotted line in 7b). It is emphasized that, for the given initial state,  $N_0(t)$  can arrive at its maximum only when  $B = B_0$ . When  $B \rightarrow \infty$ ,  $E_{gap} \rightarrow 2q \rightarrow \infty$  while  $b_1^{(1)} \rightarrow 1$  and  $b_2^{(1)} \rightarrow 0$ . Therefore  $t_p \rightarrow 0$  as shown in 7a, and  $A \rightarrow 0$  as shown in 7b, and the oscillation damps. The oscillation of  $Q_0(B, t)$  versus  $t$  is shown in Fig.8. The fact that a slight change of  $B$  around  $B_0$  leads to a great change in the population oscillation is notable.

In summary, a two-level system of cold sodium atoms has been studied. The following features are found.

(i) The system is inert to  $B$  in general, but very sensitive in a specific domain (D-o-S), where  $\Gamma_i(B)$  appears as a sharp peak, and  $E_{gap}$  appears as a dip. The locations of the D-o-S can be predicted and can be tuned by changing  $N$  and/or  $\omega$ .

(ii) When  $T$  is sufficiently low, the system is free from the interference of spatial excitation. There is a characteristic constant  $\gamma = 0.278466$  dedicated to 2-level systems. Accordingly, the upper limit of the internal energy  $U$  (relative to the g.s.) is  $\gamma k_B T$ . It implies that the  $U$  of the whole  $N$ -body system is even  $< \frac{1}{2}k_B T$ , the energy assigned to a single spatial degrees of freedom.

(iii) When  $B = B_0$  (where the dip of  $E_{gap}$  locates at),  $\bar{P}_0^{B,T}$  distinct in  $T$  converge at  $1/N$ . Once  $\bar{P}_0^{B,T}$  can be measured, the messages on  $N$ ,  $B_0$ , and thereby the dynamic parameters can be obtained.

(iv) The spin-evolution depends strongly on  $B$ . When  $B < B_{left}$ , the amplitude of oscillation is small (Fig.7). When  $B > B_{right}$ , the oscillation damps due to the sustained increasing of the  $E_{gap}$ . When  $B$  falls into the D-o-S, a strong oscillation emerges. Thereby valuable message on the dynamic parameters can be extracted.

(v) We have found a number of distinguished features for Na. The crucial point is the existence of the minimum in  $E_{gap}$ . Note that  $\langle N-1, 0, 1 | \vartheta_{N-2, N-2}^N \rangle = 0.9915$  while  $\langle N-1, 0, 1 | \vartheta_{N, N-2}^N \rangle = 0.1302$ . Therefore, when  $B$  is small, the g.s. dominated by  $\vartheta_{N-2, N-2}^N$  contains more  $\mu \neq 0$  particles than the excited state contains. Thus the increase of Zeeman energy in the g.s. is faster than that in the excited state. This leads to a decline of the gap. Such a decline will be ended at  $B = B_0$  at which  $N_0$  of both states are the same. Whereas, for Rb, the g.s. contains fewer  $\mu \neq 0$  particles. Thus the decline of the gap in accord with the increase of  $B$  does not happen. Accordingly, the minimum of the gap is located at  $B = 0$ . Hence, the 2-level systems of Rb would have completely different features.

In this paper we have not considered the interference of spatial excitation. In a recent paper it is reported that some features of a gas of Na atoms with multi-spatial-mode can be explained based on a theory independent of the spatial degrees of freedom.[9] Similar features between Fig.2 of that paper and Fig.7 of our paper are found. Nonetheless, when  $T \gtrsim T_b$ , how serious the spatial-mode would affect the spin-motion of our 2-level system deserves to be further studied.

## Acknowledgments

The project is supported by the National Basic Research Program of China (2008AA03A314, 2012CB821400, 2013CB933601), NSFC projects (11274393, 11074310, 11275279), RFDPE of China (20110171110026) and NCET-11-0547.

- 
- [1] J. Stenger, et al., Nature **396**, 345 (1998).  
 [2] M. S. Chang, Q. Qin, W. X. Zhang, L. You, and M. S. Chapman, Nature Physics **1**, 111 (2005).  
 [3] A. T. Black, E. Gomez, L. D. Turner, S. Jung, and P. D.

- Lett, Phys. Rev. Lett. **99**, 070403 (2007).  
 [4] J. Kronjäger, C. Becker, M. Brinkmann, R. Walsler, P. Navez, K. Bongs, and K. Sengstock, Phys. Rev. A **72**, 063619 (2005).

- [5] J. Kronjäger, C. Becker, P. Navez, K. Bongs, and K. Sengstock, *Phys. Rev. Lett.* **97**, 110404 (2006).
- [6] J. M. Higbie, L. E. Sadler, S. Inouye, A. P. Chikkatur, S.R. Leslie, K. L. Moore, V. Savalli, and D. M. Stamper-Kurn, *Phys. Rev. Lett.* **95**, 050401 (2005).
- [7] A. Widera, F. Gerbier, S. Föling, T. Gericke, O. Mandel, and I. Bloch, *Phys. Rev. Lett.* **95**, 190405 (2005).
- [8] A. Widera, F. Gerbier, S. Föling, T. Gericke, O. Mandel, and I. Bloch, *New J. Phys.* **8**, 152 (2006).
- [9] H. K. Pechkis, J. P. Wrubel, A. Schwettmann, P. F. Griffin, R. Barnett, E. Tiesinga, and P. D. Lett, *Phys. Rev. Lett.* **111**, 025301 (2013).
- [10] J. Katriel, *Mol. Struct.:THEOCHEM* **547**,1 (2001).
- [11] C. G. Bao and Z. B. Li, *Phys. Rev. A* **70**, 043620 (2004).
- [12] C. G. Bao and Z. B. Li, *Phys. Rev. A* **72**, 043614 (2005).
- [13] C. G. Bao, *J. Phys. A:Math. Theor.* **45**, 235002 (2012).
- [14] H. T. Quan, Z. Song, X. F. Liu, P. Zanardi, and C. P. Sun, *Phys. Rev. Lett.* **96**, 140604 (2006); W.-L. You, Y.-W. Li, and S.-J. Gu, *Phys. Rev. E* **76**, 022101 (2007).
- [15] B. Pasquiou, E. Maréchal, L. Vernac, O. Gorceix, and B. Laburthe-Tolra, *Phys. Rev. Lett.* **108**, 045307 (2012).
- [16] Z. B. Li, D. X. Yao, C. G. Bao, arXiv:1309.1933 [cond-mat,stat-mech], 2013.
- [17] Z. F. Chen, C. G. Bao, and Z. B. Li, *J. Phys. Soc. Japan*, **78**, 114002 (2009).